

# Solution for the BFKL Pomeron Calculus in zero transverse dimensions

---

**M. Kozlov\* and E. Levin†**

*Department of Particle Physics, School of Physics and Astronomy  
Raymond and Beverly Sackler Faculty of Exact Science  
Tel Aviv University, Tel Aviv, 69978, Israel*

**ABSTRACT:** In this paper the exact analytical solution is found for the BFKL Pomeron calculus in zero transverse dimensions, in which all Pomeron loops have been included. The comparison with the approximate methods of the solution is given, and it is shown, that they describe the asymptotic behaviour of the scattering amplitude quite well. In particular, the semi-classical approach is considered, which reproduces the main properties of the exact solution at large values of rapidity ( $Y \geq 12.5$ ).

**KEYWORDS:** BFKL Pomeron, Generating functional, Semi-classical solution, Sturm-Liouville problem, Exact solution .

---

\*Email: kozlov@post.tau.ac.il;

†Email: leving@post.tau.ac.il, levin@mail.desy.de;

---

## Contents

<b>1. Introduction</b>	<b>2</b>
<b>2. The equation and its general properties</b>	<b>3</b>
2.1 The equation and initial and boundary conditions.	3
2.2 General properties of the Sturm-Liouville problem	5
2.3 The algorithm for a search of the solution	7
<b>3. Analytical solution to the Sturm-Liouville problem</b>	<b>9</b>
3.1 Semi-classical approach	9
3.2 Exact solution at $u \rightarrow 1$	15
3.3 Approximate method	17
<b>4. The exact solution to the problem</b>	<b>18</b>
<b>5. Numerical estimates</b>	<b>20</b>
<b>6. Conclusions</b>	<b>21</b>
<b>7. Acknowledgments:</b>	<b>21</b>
<b>A. Appendix A: The exact semi-classical solution.</b>	<b>23</b>
<b>B. Appendix B: The exact solution as a power series in rapidity</b>	<b>25</b>
<b>C. Appendix C: The interaction procedure for the spectrum of the problem</b>	<b>27</b>

---

## 1. Introduction

It is well known that the BFKL Pomeron calculus[1, 2] gives the simplest and the most elegant approach to the high energy amplitude in QCD. This approach is based on the BFKL Pomeron [3] and the interactions between the BFKL Pomerons [4, 5, 6, 7], which are taken into account in the spirit of the Gribov Reggeon Calculus [8]. It can be written in the form of the functional integral (see Ref. [5]) and formulated in terms of the generating functional (see Refs. [9, 10, 11, 12, 13]). However, in spite of the fact that we have learned a lot about the properties of the high energy asymptotic behaviour at high energies, even the simplest case of the BFKL Pomeron in zero transverse dimension ( a toy model , see Refs. [9, 12, 13]) has not been solved<sup>1</sup> In this paper we develop the analytical approach to this problem and find the solution. We hope that this solution will help us to develop a technique for the general approach in which the amplitude depends on the size of interacting dipoles as well as on their impact parameters.

The simple toy model has some advantages which makes it a good laboratory for seeking the solutions that include the Pomeron loops. First of all, the mean field approximation [1, 2, 16, 17] for this model has a simple analytical solution [10, 11] while it is a difficult problem in the general case and we have only few analytical approaches [18, 19], therefore, we have to rely very often (too often) on the numerical solutions [20] . The JIMWLK approach[23] coincides with the Balitsky-Kovchegov [17] one in this model making our life simpler in the mean field approach.

The first corrections due to the Pomeron loops which were suggested in Ref. [21] can be easily summed in this model [22] giving a guide for the general impact of the Pomeron loops on the high energy asymptotic behaviour of the scattering amplitude.

We are aware that we can loose the important property of the QCD approach (see Refs. [24, 25, 26, 27, 28]) but we believe that the analytical solution to the simple model is a necessary step in finding more general and certainly more complicated solutions. We are certain that methods developed for solving this model, will be useful for searching for a general solution of this challenging and difficult problem.

The paper is organized as follows. In the next section we discuss the general properties of the equation that we need to solve. Being a diffusion equation this equation could be rewritten as the Sturm-Liouville equation which has a discrete spectrum. In section 3 we develop the semi-classical approach which results in finding the analytical solution to the equation. We show that this solution approaches the so called asymptotic solution at high energies. In this section we discuss the analytical solution at  $u \rightarrow 1$  which gives the transparent example of the main properties of the general solution.

In section 4 we find the general analytical solution to the problem. We state that the oblate spheroidal wave functions is the complete set of the eigenfunctions of the master equation and build the Green function as well as solution to the master equation that satisfy the initial and boundary conditions that has been discussed in section 2.

In conclusions we discuss our results and check the approximate approaches, developed for this kind of equations, against the exact solution.

---

<sup>1</sup>Some progress has been made in Refs. [13, 14, 15] and we will comment on these efforts below.

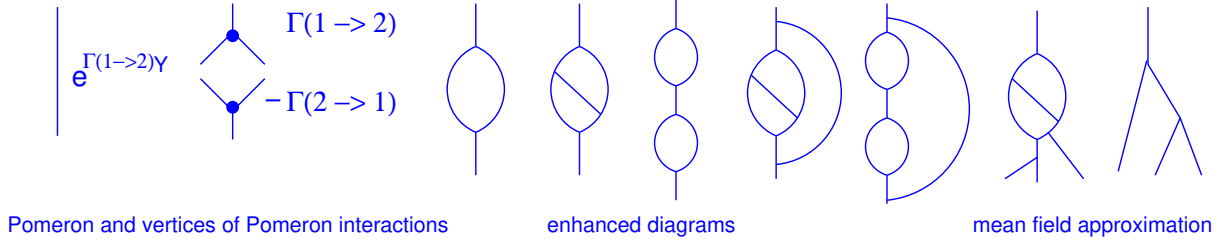


**Figure 1:** The Pomeron diagrams that are summed by Eq. (2.1). Solid lines denote the Pomerons. The first three diagrams show the Pomeron and vertices of Pomeron interaction. The next five diagrams are the examples of so called enhanced diagrams which we are going to sum in this paper. The last two diagrams give the example of the Pomeron diagrams in the mean field approximation.

## 2. The equation and its general properties

### 2.1 The equation and initial and boundary conditions.

In the toy model the equation for the generating functional<sup>2</sup> has a simple form [9, 12, 13]

$$\frac{\partial Z}{\partial \mathcal{Y}} = u(1-u) \left( -\kappa \frac{\partial Z}{\partial u} + \frac{\partial^2 Z}{(\partial u)^2} \right) \quad (2.1)$$

where  $\mathcal{Y} = \Gamma(2 \rightarrow 1)Y = (\Gamma(1 \rightarrow 2)/\kappa)Y$  with vertex  $\Gamma(2 \rightarrow 1)$  which describes a merging of two dipoles into one dipole.  $\kappa$  is the large parameter of our problem and it is equal to

$$\kappa = \frac{\Gamma(1 \rightarrow 2)}{\Gamma(2 \rightarrow 1)} = \frac{1}{\alpha_S^2} \gg 1 \quad (2.2)$$

where  $\alpha_S$  is QCD coupling and  $\Gamma(1 \rightarrow 2) = (N_c/\pi)\alpha_S = \bar{\alpha}_S$  is the vertex for the decay of the dipole into two dipoles. The order of these vertices  $\Gamma(1 \rightarrow 2)$  and  $\Gamma(2 \rightarrow 1)$  are chosen from the general equation for the generating functional in QCD (see Ref. [12] for example).

Eq. (2.1) is a typical diffusion equation with the diffusion coefficient that depends on variable  $u$ . We need to add an initial and boundary condition to solve such kind of equation. Generally, this equation describes the interaction between Pomerons with intercept  $\Delta_P = \Gamma(1 \rightarrow 2) = \bar{\alpha}_S$ . The Pomeron diagrams that describes Eq. (2.1) are shown in Fig. 1.

In this paper we are going to calculate the sum of enhanced diagrams (see Fig. 1) and for them we have the following initial condition<sup>3</sup>

$$Z(Y=0; u) = u \quad (2.3)$$

<sup>2</sup>Actually for the toy model, in which there is no dependence on the sizes of interacting dipoles, the generating functional degenerates to the generating function.

<sup>3</sup>In Eq. (2.3) as well everywhere below we use the notation  $Y$  for  $\mathcal{Y}$ . Hopefully it will not lead to troubles in understanding.

Since the physical meaning of  $Z$  is

$$Z(Y; u) = \sum_{n=0}^{\infty} P_n(Y) u^n \quad (2.4)$$

where  $P_n(Y)$  is the probability to find  $n$ -dipoles (or/and  $n$ -Pomerons) at rapidity  $Y$ . Therefore, Eq. (2.3) means that at low energies we have only one Pomeron.

The master equation (see Eq. (2.1)) describes Markov's chain for the probabilities  $P_N(Y)$ , namely [24, 12]

$$\begin{aligned} \frac{dP_n(Y)}{dY} = & -\Gamma(1 \rightarrow 2) n P_n(Y) + \Gamma(1 \rightarrow 2) (n-1) P_{n-1}(Y) \\ & - \Gamma(2 \rightarrow 1) \frac{n(n-1)}{2} P_n(Y) + \Gamma(2 \rightarrow 1) \frac{n(n-1)}{2} P_{n+1}(Y) \end{aligned} \quad (2.5)$$

Eq. (2.5) has a simple structure: for every process of dipole splitting or merging we see two terms. The first one with the negative sign describes a decrease of probability  $P_n$  due to the process of splitting or merging of dipoles. The second term with positive sign is responsible for the increase of the probability due to the same processes of dipole interactions.]

The boundary conditions are very simple

$$Z(Y; u = 1) = \sum_{n=0}^{\infty} P_n(Y) = 1 \quad (2.6)$$

which directly follows from Eq. (2.4) and express the conservation of probabilities, saying that the total probability is equal to unity at any value of rapidity.

Using the Laplace transform

$$Z(Y; u) = \int_{a-i\infty}^{a+i\infty} \frac{d\omega}{2\pi i} Z(\omega; u) e^{\omega Y} \quad (2.7)$$

we can reduce Eq. (2.1) to the following equation

$$\frac{\omega}{u(1-u)} Z(\omega; u) = -\kappa Z'_u(\omega; u) + Z''_{u,u}(\omega; u) \quad (2.8)$$

Introducing new functions

$$s(u) \equiv \frac{1}{u(1-u)} e^{-\kappa u}; \quad \text{and} \quad p(u) \equiv e^{-\kappa u}; \quad (2.9)$$

we can reduce Eq. (2.8) to the typical Sturm-Liouville equation [29, 30]

$$-s(u) \omega Z(\omega, u) + \frac{d}{du} (p(u) Z_u(\omega, u)) = 0 \quad (2.10)$$

## 2.2 General properties of the Sturm-Liouville problem

It is very instructive to remind ourselves of the general properties of the Sturm-Liouville problem which has been studied by mathematicians for a long time [29, 30].

1. Eq. (2.10) has the infinite set of the eigenvalues  $\omega_n = -\lambda_n$ . All  $\lambda_n$  are real and can be ordered so that  $\lambda_1 < \lambda_2 < \lambda_3$  with  $\lambda_n \rightarrow +\infty$ . Therefore, there can exist only a finite number of negative  $\lambda_n$ . The multiplicity of each eigenvalue is equal to 1;
2. The eigenvalues are determined up to a constant multiplier. Each eigenfunction  $Z_n(u)$  has exactly  $n - 1$  zeroes in the interval  $(0, 1)$ ;
3. Eigenfunctions  $Z_n(u)$  and  $Z_m(u)$  are orthogonal with weight  $s(u)$ , namely,

$$\int_0^1 du s(u) Z_n(u) Z_m(u) = 0 \quad \text{for } n \neq m \quad (2.11)$$

4. An arbitrary function  $F(u)$ , that has a continuous derivative and satisfies the boundary conditions of the Sturm-Liouville problem (in other words, a function that we, as physicists, want to find), can be expanded into absolute and uniformly convergent series in eigenfunctions:

$$F(u) = \sum_{n=1}^{\infty} F_n Z_n(u); \quad \text{where } F_n = \frac{1}{\|Z_n\|} \int_0^1 du F(u) Z_n(u) \quad (2.12)$$

where

$$\|Z_n\|^2 = \int_0^1 du s(u) Z_n^2(u) \quad (2.13)$$

5. For Eq. (2.10) there are no negative eigenvalues  $\lambda_n$  and  $\lambda_1 = 0$  is the least eigenvalue, to which there corresponds the eigenfunction  $Z_0(u) = \text{Constant}$ ;
6. The following asymptotic relation holds for large eigenvalues as  $n \rightarrow \infty$ :

$$\lambda_n = \frac{\pi^2 n^2}{\Delta^2} + O(1); \quad \text{where } \Delta = \int_0^1 \sqrt{\frac{s(u)}{p(u)}} du; \quad (2.14)$$

7. In our case (see Eq. (2.9))

$$\Delta = \int_0^1 \frac{du'}{\sqrt{u'(1-u')}} = \pi, \quad (2.15)$$

and, therefore, at large  $n$

$$\lambda_n = n^2 \quad (2.16)$$

In Appendix C we compare this asymptotic spectrum with the spectrum of the exact solution as well as with the perturbation procedure to calculate it, given in the next section.

8. In our case we can use Eq. (2.16) and Eq. (2.14) for  $n \gg 1$  to estimate not only the values of  $\lambda_n$  but also to find the corresponding eigenfunctions. These eigenfunctions have the following form:

$$\frac{Z_n(u)}{\|Z_n\|} = \left( \frac{4}{\pi^2} u(1-u) \right)^{\frac{1}{4}} e^{\frac{\kappa}{2}u} \sin(n\Theta(u)) + O\left(\frac{1}{n}\right) \quad (2.17)$$

where

$$\Theta(u) = - \int_u^1 \frac{du'}{\sqrt{u'(1-u')}} = -\frac{\pi}{2} - \arcsin(1-2u) \quad (2.18)$$

Introducing a more general equation than Eq. (2.10), namely,

$$s(u) \frac{\partial Z(Y, u)}{\partial Y} = \frac{d}{du} (p(u) Z_u(\omega, u)) + \Phi(Y, u) \quad (2.19)$$

where  $\Phi(Y, u)$  is a given function. We can find a general solution to this equation with the initial condition:

$$Z(Y=0, u) = f(u) \quad (2.20)$$

and with the boundary conditions:

$$Z(Y, u=0) = 0; \quad (2.21)$$

$$Z(Y, u=1) = 1; \quad (2.22)$$

The form of this solution is (see section **1.8.9** in Ref. [30])

$$\begin{aligned} Z(Y, u) &= \int_0^Y dY' \int_0^1 d\xi \Phi(Y', \xi) G(Y-Y'; u, \xi) + \int_0^1 d\xi s(\xi) f(\xi) G(Y; u, \xi) \\ &+ p(u=1) \int_0^Y dY' \frac{\partial G(Y-Y'; u, \xi)}{\partial \xi} \Big|_{\xi=1} \end{aligned} \quad (2.23)$$

where the Green function of this equation is equal to

$$G(Y; u, \xi) = \sum_{n=1}^{\infty} \frac{Z_n(u) Z_n(\xi)}{\|Z_n\|^2} e^{-\lambda_n Y} \quad (2.24)$$

where  $Z_n$  are the eigenfunction of Eq. (2.10) with the boundary conditions

$$Z_n(Y, u=0) = 0; \quad Z_n(Y, u=1) = 0; \quad (2.25)$$

One can see that we know a lot about the properties of the master equation.

### 2.3 The algorithm for a search of the solution

The general formulae, given in the previous section, leads to a definite algorithm for numerical calculations. In the first stage of this algorithm we can use the eigenvalues given by Eq. (2.16), and the eigenfunctions from Eq. (2.17). The Green function has the form

$$G_{\infty}(Y; u, \xi) = \frac{2}{\pi} \sqrt{\sin \Theta(u) \sin \Theta(\xi)} e^{\frac{\kappa}{2}(u+\xi)} \sum_{n=-\infty}^{n=\infty} \exp(i \{ \Theta(u) - \Theta(\xi) \}) e^{-n^2 Y} \quad (2.26)$$

The solution can be found from Eq. (2.23) and it has the form

$$\begin{aligned} Z_{\infty}(Y, u) = & \int_0^Y dY' \int_{-\pi}^0 d\Theta' \frac{\frac{1}{2}(\cos \Theta' + 1)}{\sin \Theta'} e^{-\kappa u} G_{\infty}(Y; u, \xi) - \\ & - \int_0^Y dY' \frac{\partial G_{\infty}(Y - Y'; u, \xi)}{\partial \xi} \Big|_{\xi=1} \end{aligned} \quad (2.27)$$

In the next stage of the algorithm we are searching for the solution in the form

$$Z(Y, u) = \Delta Z(Y, u) + Z_{\infty}(Y, u) \quad (2.28)$$

and for  $\Delta Z(Y, u)$  we obtain the following equation

$$-s(u) \omega \Delta Z(Y, u) + L(\Delta Z(Y, u)) + L(Z_{\infty}(Y, u)) \quad (2.29)$$

where we denote by  $L$  the Sturm-Liouville operator, namely  $L = \frac{d}{du} (p(u) \frac{d}{du})$ .

One can see that Eq. (2.29) has the form of Eq. (2.19) with  $\Phi(Y, u) = L(Z_{\infty}(Y, u))$ . Using Eq. (2.23) we can find  $\Delta Z(Y, u)$ . Repeating this procedure several times we will obtain the numerical solution to the problem. However, the procedure would be better converged if we could determine the eigenvalues of the problem at small values of  $n$ . Below we suggest two approximations that allows us to approach small values of  $n$ .

The algorithm described above has a very simple meaning if we re-write our equation as a Schroedinger-type equation. It is easy to see that the search for  $Z_{\infty}(Y, u)$  of Eq. (2.27) can be simplified if we introduce a new function  $T$

$$Z(Y, u) = T(Y, \Theta) e^{\frac{\kappa}{2} u} \quad (2.30)$$

For this function we can rewrite Eq. (2.23) in the very convenient form for the function  $T(Y, \Theta)$  introducing a new variable  $\Theta$  (see Eq. (2.18) instead of  $u$ ).

$$\frac{\omega}{\sin \Theta} T(\omega, \Theta) = -\frac{\kappa^2}{4} \sin \Theta T(\omega, \Theta) + \frac{d}{d\Theta} \frac{1}{\sin \Theta} \frac{d T(\omega, \Theta)}{d\Theta} \quad (2.31)$$

which is a generalized Sturm - Liouville equation of the form



$$s(\Theta) \frac{\partial T(Y, \Theta)}{\partial Y} = \frac{\partial}{\partial \Theta} p(\Theta) \frac{\partial T(\omega, \Theta)}{\partial \Theta} - q(\Theta) T(\omega, \Theta) \quad (2.32)$$

with

$$s(\Theta) = 1/\sin \Theta; \quad p(\Theta) = 1/\sin \Theta; \quad q(\Theta) = \frac{\kappa^2}{4} \sin \Theta \quad (2.33)$$

Eq. (2.32) allows us to find corrections of the order of  $1/n^2$  to the spectrum of the Sturm - Liouville operator. Indeed,  $\lambda_n$  is equal to (see section **1.8.9** in Ref. [30])

$$\sqrt{\lambda_n} = n + \frac{1}{\pi n} Q(0, -\pi) + O\left(\frac{1}{n^2}\right) \quad (2.34)$$

where

$$Q(\Theta, \Theta') = \frac{1}{2} \int_{\Theta'}^{\Theta} d\Theta'' q(\Theta'') = \frac{\kappa}{4} \{\cos \Theta' - \cos \Theta\} \quad (2.35)$$

The estimate for the eigenfunctions looks as follows

$$T_n(\Theta) = \sin(n\Theta) - \frac{\kappa^2}{4\pi n} \{2\Theta + \pi(1 - \cos \Theta)\} \cos(n\Theta) + O\left(\frac{1}{n^2}\right) \quad (2.36)$$

Eq. (2.31) can be re-written as a Schroedinger-type equation:

$$\frac{d^2 \Psi}{(d\Theta)^2} + (E - U(\Theta)) \Psi = 0. \quad (2.37)$$

Indeed, Eq. (2.31) has the equivalent form

$$\omega T = -\frac{\kappa^2}{4} \sin^2 \Theta T_{\Theta} - \cot \Theta T_{\Theta} + T_{\Theta\Theta} \quad (2.38)$$

Introducing

$$T = \phi(\Theta) \Psi(\Theta) \quad \text{with} \quad \phi(\Theta) = \sqrt{\sin \Theta} \quad (2.39)$$

we obtain for  $\Psi$  the Schroedinger equation with

$$E = -\omega; \quad \text{and} \quad (2.40)$$

$$U(\Theta) = \frac{\kappa^2}{4} \sin^2 \Theta + \frac{1}{4} (2 + 3 \cot^2 \Theta);$$

In Fig. 2 we plot this potential. One can see that for large  $\kappa$  it has a typical two minima form with the maximum at  $\Theta = \pi/2$  while at  $\Theta \rightarrow 0$  and  $\Theta \rightarrow \pi$   $U(\Theta)$  increases approaching infinity.

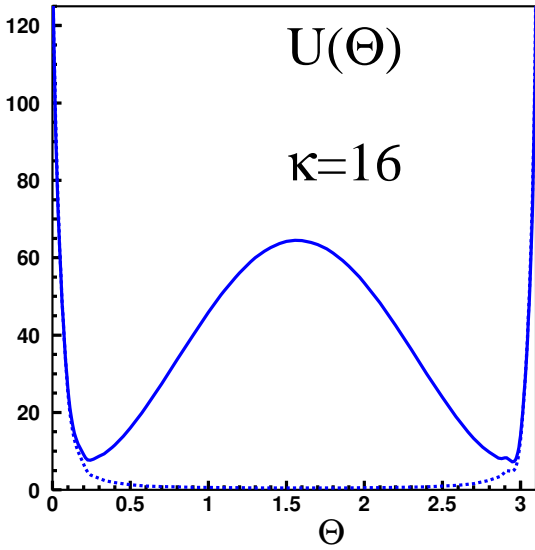


**Figure 2:** The potential energy  $U(\Theta)$  of Eq. (2.40) versus  $\Theta$  at  $\kappa=16$ , . The dashed line shows the potential  $U(\Theta) - (\kappa^2/4) \sin^2 \Theta$  which corresponds to the set of the eigenfunctions given by Eq. (2.17).

Therefore, for large energy excitation we can replace this potential by the rectangular-well potential with the wave functions given by Eq. (2.17) with the spectrum of Eq. (2.14).

Actually we can reduce Eq. (2.37) to the Schroedinger equation with the simplified potential, namely,

$$\frac{d^2\Psi}{(d\Theta)^2} + \left(E - \frac{\kappa^2}{4} \sin^2(\Theta)\right) \Psi = 0; \quad \text{with} \quad \Psi(\Theta=0) = \Psi(\Theta=\pi) = 0 \quad (2.41)$$

This equation replace the potential  $U(\Theta) - \frac{\kappa^2}{4} \sin^2(\Theta)$  (see the dashed line in Fig. 2) by the rectangular-well potential.

The fact that we have two minima potential leads to the asymptotic behaviour of the amplitude which is determined by the asymptotic solution of Eq. (2.8) for  $\omega = 0$  (see Refs.[13, 38, 39]), namely,

$$Z_{asymp}(Y = \infty, u) = \frac{1 - e^{\kappa u}}{1 - e^{\kappa}} \quad (2.42)$$

which satisfy both boundary conditions:  $Z_{asymp}(u=0) = 0$  and  $Z_{asymp}(u=1) = 1$ .

In section 4 we will give the exact analytical solution to the master equation and we postpone until this section our discussion of this Schroedinger-type of the equation. However, this equation (see Eq. (2.37)) allows us to use the usual perturbative approach for the numerical solutions. For example we can represent the potential  $U(\Theta)$  of Eq. (2.40) in the form

$$U(\Theta) = U_0(\Theta) + V(\Theta) \quad (2.43)$$

and solve Eq. (2.37) with  $U_0$  exactly. Considering  $V(\Theta)$  as being small we can develop the usual perturbation approach in quantum mechanics for a numerical solution of the equation.

The other way to find a good first approximation for searching  $Z_\infty$  is to use the semi-classical approach which we consider below.

### 3. Analytical solution to the Sturm-Liouville problem

#### 3.1 Semi-classical approach

In our master equation (see Eq. (2.8)) we have a natural large parameter:  $\kappa$  (see Eq. (2.2)). We wish to use this parameter to develop a semi-classical approach to the master equation. We assume that

$$Z(\omega; u) = e^{\phi(\omega; u)} \quad \text{where} \quad \phi''_{u,u} \ll (\phi'_u)^2 \quad (3.1)$$

Substituting Eq. (3.1) into Eq. (2.8) one can reduce this equation to the form

$$\frac{\omega}{u(1-u)} = -\kappa \phi'_u + (\phi'_u)^2 \quad (3.2)$$

Solving Eq. (3.2) we obtain

$$\frac{d\phi_u^\pm}{du} = \frac{\kappa}{2} \left( 1 \pm \sqrt{1 + \frac{4\omega}{\kappa^2 u(1-u)}} \right) \quad (3.3)$$

and

$$\phi^\pm(\omega; u) = - \int_u^1 \phi_{u'}^{\pm, \prime}(\omega; u') du' \quad (3.4)$$

The general solution to Eq. (3.1) has the form

$$Z(Y; u) = \int_{a-i\infty}^{a+i\infty} \frac{d\omega}{2\pi i} e^{\omega \mathcal{Y}} \left\{ \Phi^{(-)}(\omega) e^{\phi^-(\omega, u)} + \Phi^{(+)}(\omega) e^{\phi^+(\omega, u)} \right\} \quad (3.5)$$

where functions  $\Phi^{(-)}(\omega)$  and  $\Phi^{(+)}(\omega)$  should be found from initial and boundary conditions (see Eq. (2.3) and Eq. (2.6)).  $\mathcal{Y} = \Gamma(2 \rightarrow 1) Y$ .

The contour of integration (contour  $C$  in Fig. 3) over  $\omega$  is situated to the right of the singularities as it is shown in Fig. 3. As we have discussed the general structure of the singularities looks as follows. We have no singularities for positive  $\omega = \omega_n^+ > 0$ . It looks strange since one can see from Eq. (3.3) that we have a restricted number of singularities for positive  $\omega = \omega_n^+ > 0$ . However, since the contour of integration  $C$  in Fig. 3 is placed between  $\omega_0 = 0$  and  $\omega = \omega_1^+$ , we can close it to the right semi-plane (see contour  $C_1$  in Fig. 3). Therefore, the singularities  $\omega_n^+$  does not contribute to the integral of Eq. (3.5).

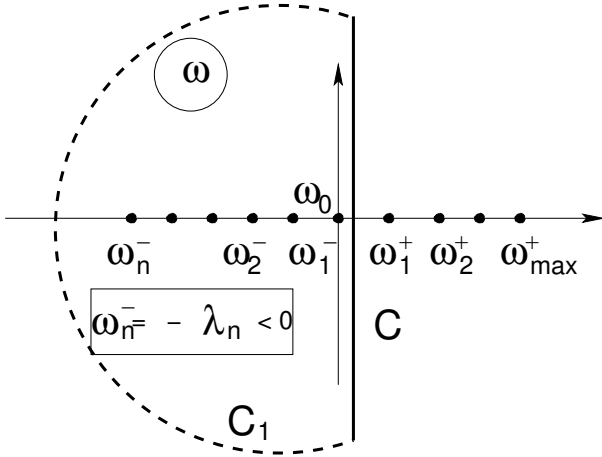


**Figure 3:** The contours of integration over  $\omega$  in Eq. (3.5). All singularities are located along real negative real axis ( $\omega_n = -\lambda_n < 0$ )

Ref. [10], for example) one can see that all positive singularities  $\omega^+$  in Fig. 3) are the singularities of  $\Phi^{(-)}$  while  $\Phi^{(+)}$  has the singularities at the negative values of  $\omega$ . Therefore, the only singularities that we need to take into account are those that are described by Eq. (3.6).

The analytical function for Eq. (3.4) is written in the appendix A while here we will discuss this function in two different limits:  $\frac{\omega}{\kappa^2 u(1-u)} \ll 1$  and  $\frac{\omega}{\kappa^2 u(1-u)} \gg 1$ .

For  $\frac{\omega}{\kappa^2 u(1-u)} \ll 1$  we have for function  $\phi^\pm(\omega; u)$  the following expression

$$\phi^+(\omega; u) = \kappa(u-1) + \frac{\omega}{\kappa} \ln\left(\frac{u}{1-u}\right) \quad (3.6)$$

$$\phi^-(\omega; u) = -\frac{\omega}{\kappa} \ln\left(\frac{u}{1-u}\right); \quad (3.7)$$

It is easy to see that  $\phi^+(\omega; u)$  of Eq. (3.6) corresponds to the solution which survives at  $\kappa \rightarrow \infty$  which describes the case of the mean field approach. Analyzing the mean field solution (see

For  $\omega \approx \kappa^2$  we need to expand the exact formulae for  $\phi^\pm(\omega, u)$  in the kinematic region. For  $\frac{\omega}{\kappa^2 u(1-u)} \gg 1$ . In this region  $\phi^\pm(\omega, u)$  are equal to

$$\phi^\pm(\omega, u) = \frac{\kappa}{2}(u-1) \pm i\sqrt{|\omega|} \Theta(u) = \frac{\kappa}{2}(u-1) \pm i\mu_n \Theta(u) \quad (3.8)$$

where  $\Theta$  is given by Eq. (2.18) and  $\omega_n = -\lambda_n = -\mu_n^2$ .

Therefore, in both branches  $\phi^\pm$  we have singularities at negative  $\omega$  and from estimates of Eq. (2.16) we know that  $\lambda_n = n$ .

Using simple relations between variables  $u$  and  $\Theta$

$$u-1 = \frac{1}{2}(\cos \Theta - 1); \quad u = \frac{1}{2}(\cos \Theta + 1), \quad (3.9)$$

we can rewrite  $\exp(\phi^\pm(\omega, u))$  in the form

$$\exp(\phi^\pm(\omega_n = -\lambda_n = -\mu_n^2, u)) = \exp\left(\frac{\kappa}{8}\left[-2 + \zeta + \frac{1}{\zeta}\right]\right) \zeta^{\pm\mu_n} \quad (3.10)$$

where we introduce new variable

$$\zeta = e^{i\Theta} \quad (3.11)$$

It is obvious from Eq. (3.8) that  $\zeta^n$  is the eigenfunction of our master equation at large values of  $\omega$  ( $\omega \geq \kappa$ ). However, the eigenfunctions that satisfy the boundary conditions of Eq. (2.25) are

$$Z_n(\Theta) = \sin(n\Theta) \quad (3.12)$$

These functions form the complete set of functions in the interval  $0 \leq u \leq 1$ . In other words, the approximation of Eq. (2.16) turns out to be exact in our semi-classical approach. Having this fact in mind, we can find function  $\Phi^{(\pm)}(\omega)$  in Eq. (3.5) from the initial condition of Eq. (2.3).

Functions  $\zeta^n$  are eigenfunctions of Eq. (2.31) in which we neglect the first term in the r.h.s. and the second one is modified assuming that

$$\frac{d}{d\Theta} \frac{1}{\sin \Theta} \frac{dT(\omega, \Theta)}{d\Theta} \text{ is replaced by } \frac{1}{\sin \Theta} \left( \frac{dT(\omega, \Theta)}{d\Theta} \right)^2.$$

In this approximation Eq. (2.31) reduces to

$$\omega T(\omega, \Theta) = \frac{d^2 T(\omega, \Theta)}{d\Theta^2} \quad (3.13)$$

It is easy to see that Eq. (3.8) gives the eigenfunctions of this equation.

The Green function (for  $T(Y, \Theta)$ ) of this equation has a very simple form, namely

$$G_\infty^{SC}(Y; \Theta, \Theta') = \frac{1}{\pi} e^{\frac{\kappa}{2} + \frac{\kappa}{4} [\cos \Theta + \cos \Theta']} \sum_{n=1}^{\infty} \sin(n\Theta) \sin(n\Theta') \quad (3.14)$$

and the initial conditions have the form

$$T(Y=0, \Theta) = \frac{1}{2}(1 + \cos \Theta) \exp\left(-\frac{\kappa}{4}(1 + \cos \Theta)\right) \quad (3.15)$$

Using this Green function we obtain the semi-classical solution in the form

$$Z_{\infty}^{SC} = \frac{1}{\pi} \sum_{n=-\infty}^{\infty} \left\{ e^{-n^2 Y} e^{\frac{\kappa}{2} u} \sin(n \Theta) \int_{-\pi}^0 d\Theta' \sin(n \Theta') \frac{1}{2}(1 + \cos \Theta') \exp\left(-\frac{\kappa}{4}(1 + \cos \Theta')\right) \right\} \quad (3.16)$$

The integral over  $\Theta'$  could be taken using the generating function for the modified Bessel function of the first kind ( see formula **9.6.33** in Ref.[32])

$$\exp\left(\frac{\kappa}{4} \cos \Theta\right) = \sum_{n=-\infty}^{\infty} I_n\left(\frac{\kappa}{4}\right) e^{i n \Theta} \quad (3.17)$$

and the expression for simple integral

$$\int_{-\pi}^0 d\Theta' \cos(n\Theta') \sin(k\Theta') = \frac{k(1 - (-1)^{n+k})}{k^2 - n^2} \quad (3.18)$$

From Eq. (3.17) and Eq. (3.18) one can derive that

$$\begin{aligned} C(n, \kappa) &= \int_{-\pi}^0 d\Theta' \sin(n\Theta') \frac{1}{2}(1 + \cos \Theta') \exp\left(-\frac{\kappa}{4}(1 + \cos \Theta')\right) = \\ &= \frac{1}{4} \sum_{m=0}^{\infty} \exp(-\kappa/4) (I_{m+1}(-\kappa/4) + I_{m-1}(-\kappa/4) + 2I_m(-\kappa/4)) \frac{n(1 - (-1)^{n+m})}{n^2 - m^2} \end{aligned} \quad (3.19)$$

Substituting Eq. (3.19) into Eq. (3.16) we obtain

$$Z_{\infty}^{SC} = \frac{1}{\pi} e^{\frac{\kappa}{2}(u-1)} \left( C(0, k) + 2 \sum_{n=1}^{\infty} \left\{ e^{-n^2 Y} e^{\frac{\kappa}{2} u} \sin(n \Theta) C(n, \kappa) \right\} \right) \quad (3.20)$$

However, this expression for  $Z_{\infty}^{SC}$  has two disadvantages: (i) we approximate  $\omega_n = -n^2$  even at small values of  $n$  where we know that our spectrum is different (see Eq. (3.6) and Eq. (3.7)); and (ii)  $Z_{\infty}^{SC}(Y, u=1) \neq 1$  ( actually  $Z_{\infty}^{SC}(Y, u=1) = 0$ ).

The set of eigenfunction at small values of  $n$  is clear from Eq. (3.6) and Eq. (3.7), namely,

$$Z_n(u) = \begin{cases} \text{for } u \geq \frac{1}{2} & e^{\kappa(u-1)} \tau^n = \exp\left(\kappa \frac{\tau}{1-\tau}\right) \tau^n \text{ where } \tau = \frac{u-1}{u} \\ \text{for } u \leq \frac{1}{2} & \tau^n \text{ where } \tau = \frac{u}{u-1} \end{cases} \quad (3.21)$$

The fact that we have two different sets of the eigenfunctions for  $u \geq 1/2$  and  $u \leq 1/2$ , directly comes from the contour integral of Eq. (3.5) and the expressions of Eq. (3.6) and Eq. (3.7) for functions  $\phi^+$  and  $\phi^-$ . Indeed, for  $u \geq 1/2$   $\ln(u/(1-u))$  is positive and we can close the contour in Eq. (3.5) to the left semi-plane for  $\phi^+$ . For  $u \leq 1/2$  this log is negative and we have to use  $\phi^-$  for negative values of  $\omega$ . Recall, that we know from the general properties of the Sturm-Liouville equation that only negative  $\omega$  contribute.

The value of  $\omega_n = -\lambda_n$  for the eigenfunctions of Eq. (3.21) is equal to

$$\lambda_n = \kappa n \quad (3.22)$$

Coefficients  $C(n, \kappa)$  we can find using the following series

$$u \exp(-\kappa(u-1)) = \frac{1}{1-\tau} \exp\left(-\kappa \frac{\tau}{\tau-1}\right) = \sum_{n=0}^{\infty} L_n(\kappa) \tau^n \quad (3.23)$$

where  $L_n(\kappa)$  is the Laguerre polynomial (see Ref.[31]).

One can see that  $C(n, \kappa) = L_n(\kappa)$ .

We suggest to build the Green function considering for all  $\lambda_n \leq \kappa^2$  the set of the eigenfunction given by Eq. (3.21) while for  $\lambda_n > \kappa^2$  we use the set of Eq. (3.12).

It means that our Green function has the form

$$\begin{aligned} G^{SC}(Y; u, \xi) &= \exp(\kappa(u + \xi - 2)) \sum_{n=0}^{n=[\kappa]1} \tau(u) \tau(\xi) e^{-n \kappa Y} \\ &+ \exp\left(\frac{\kappa}{2}(u + \xi - 2)\right) \sum_{n=[\kappa]+2}^{\infty} \sin(\Theta(u)) \sin(\Theta(\xi)) \end{aligned} \quad (3.24)$$

which leads to the generating function in the form

$$\begin{aligned} Z^{SC}(Y; u) &= \Theta\left(u \geq \frac{1}{2}\right) \exp(\kappa(u-1)) \sum_{n=0}^{n=[\kappa]+1} \tau(u)^n L_n(\kappa) e^{-n \kappa Y} \\ &+ \Theta\left(u \leq \frac{1}{2}\right) \sum_{n=0}^{n=[\kappa]+1} \tau(u)^n e^{-n \kappa Y} + \exp\left(\frac{\kappa}{2}(u-1)\right) \sum_{n=[\kappa]+2}^{\infty} \sin(\Theta(u)) C(n, \kappa) e^{-n^2 Y} \end{aligned} \quad (3.25)$$

This solution has two problems which cannot be solved analytically: a dependence of the separation parameter between large and small  $n$  which was taken in Eq. (3.25) to be equal to  $[\kappa] + 1$  and rather complicated expression for  $C(n, \kappa)$  (see Eq. (3.19)) which does not allow us to make all calculation analytically. We investigated both problems computing Eq. (3.25) numerically for different separation parameters. It turns out that the answer is very insensitive to the exact value of the separation parameter if only we take it around  $\kappa$ . Actually, the value of this parameter we can find comparing exact semi-classical functions  $\phi^\pm$  with our approximate ones ( see Appendix A, where we discuss the exact functions).

The behaviour of the scattering amplitude is illustrated in Fig. 4 as a function of rapidity  $Y$ . In Fig. 5 one can see the  $u$  dependence of our solution at large values of rapidity  $Y$ . This behaviour confirms the expectation that has been discussed in Ref. [13], that at high energy our master equation predicts the gray disc behaviour for the scattering amplitude.

We check the accuracy of the semi-classical solution by calculating the following function:

$$\Delta(Y, u) = \frac{\left( \frac{\partial}{\partial Y} + \kappa u(1-u) \frac{\partial}{\partial u} - u(1-u) \frac{\partial^2}{(\partial u)^2} \right) Z^{SC}(Y, u)}{\text{minimal separate term of the numerator}} \quad (3.26)$$

As we have expected the semi-classical approach is rather bad at small values of  $Y \leq 0.05$  leading to  $\Delta(Y, u) \approx 40\%$  for  $u \approx 0.5$ . However, for large values of  $Y$  ( $Y > 0.1$ ) the accuracy is better than 10 % for all values of  $u$ . It should be stressed that for  $u > 0.8$  in the entire kinematic region of  $Y$  the accuracy is not worse than 10%. All estimates were done for  $\kappa = 16$ . This fact is very encouraging since the scattering amplitude  $N$  can be calculated in the following way [17]

$$N(Y, \gamma) = 1 - Z(Y, u = 1 - \gamma) \quad (3.27)$$

where  $\gamma$  is the scattering amplitude at low energy ( $Y=0$ ). In our QCD motivated model  $\gamma \approx 1/\kappa \ll 1$ . Therefore, we are interested only in the values of  $u$  that are close to unity ( $u \rightarrow 1$ ), where the semi-classical approach works quite well.

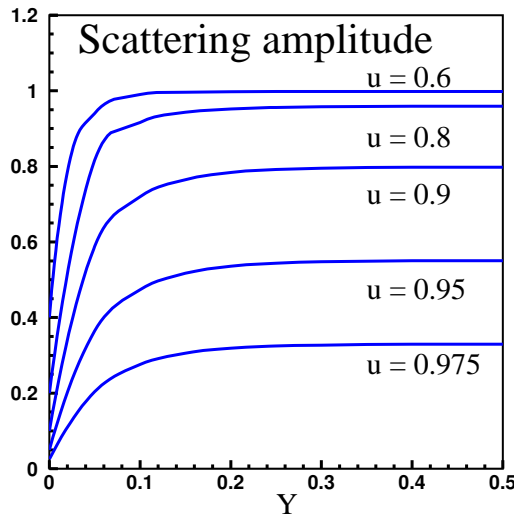


**Figure 4:** The dependence of the scattering amplitude versus  $Y \equiv \mathcal{Y}$  at fixed  $\kappa = 16$ .

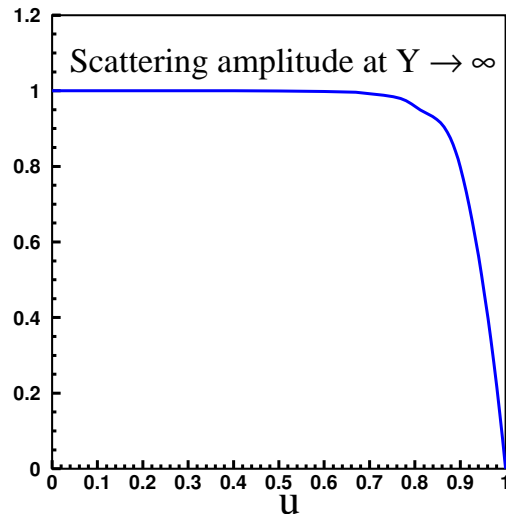


**Figure 5:** The asymptotic dependence of the scattering amplitude (see Eq. (3.25)) versus  $u$  at fixed  $\kappa = 16$ .

However, in the next section we develop a better analytical approach for such  $u$ .

### 3.2 Exact solution at $u \rightarrow 1$

To check that the eigenvalues in the region of small  $\omega$  is determined by Eq. (3.22) we develop a different analytical approach. In the vicinity of  $u = 1$  we can replace Eq. (2.1) by the following equation:

$$\frac{\partial Z}{\partial \mathcal{Y}} = (1 - u) \left( -\kappa \frac{\partial Z}{\partial u} + u \frac{\partial^2 Z}{(\partial u)^2} \right) \quad (3.28)$$

For  $Z(\omega, u)$  Eq. (3.28) reduces to the form

$$\omega Z(\omega, u) = -\kappa(1 - u) Z_u(\omega, u) + u(1 - u) Z_{uu}(\omega, u) \quad (3.29)$$

The solution to Eq. (3.29) is the Gauss's hypergeometric function

$$Z(\omega, u) = u^{1+\kappa} {}_2F_1(\alpha, \beta, \gamma, u) \quad (3.30)$$

(see formula **9.151** in Ref. [31]) with the following parameters

$$\begin{aligned} \alpha &= \frac{1}{2}(1 + \kappa) + \frac{1}{2}\sqrt{(1 + \kappa)^2 - 4\omega}; \\ \beta &= \frac{1}{2}(1 + \kappa) - \frac{1}{2}\sqrt{(1 + \kappa)^2 - 4\omega}; \\ \gamma &= \kappa + 2; \end{aligned} \quad (3.31)$$

The generating function that satisfies the boundary condition  $Z(Y, u = 1) = 1$  is equal to

$$Z(\omega, u) = u^{1+\kappa} \frac{1}{\omega} \frac{{}_2F_1(\alpha, \beta, \gamma, u)}{{}_2F_1(\alpha, \beta, \gamma, u = 1)} \quad (3.32)$$

Since (see formula **9.122** in Ref. [31])

$${}_2F_1(\alpha, \beta, \gamma, u = 1) = \frac{\Gamma(\gamma) \Gamma(1)}{\Gamma(\gamma - \alpha) \Gamma(\gamma - \beta)} \quad (3.33)$$

The eigenvalues stem from the poles of  $\Gamma(\gamma - \alpha)$  (or  $\Gamma(\gamma - \beta)$ ), namely, from the equation

$$\gamma - \alpha = -n; \quad \text{which gives} \quad \omega_n = -\lambda_n = -n^2 - n(1 + \kappa); \quad (3.34)$$

This equation leads to a smooth transition between large and small values of  $n$  supporting our semi-classical formula. Substituting Eq. (3.32) in Eq. (3.5) one can find the eigenfunction of our equation. They have the following form

$$Z_n(u) = \frac{1}{\|Z_n\|^2} u^\kappa P_n^{-1, 1+\kappa}(2u - 1) \quad (3.35)$$

where  $P_n^{-1, 1+\kappa}$  are the Jacobi polynomials ( see sections **8.960 - 8.967** in Ref. [31]).

The normalization of function  $Z_n$  in Eq. (3.35) is obvious since

$$\|Z_n\|^2 = \quad (3.36)$$



$$\int_0^1 du \frac{u^{1+\kappa}}{1-u} (P_n^{-1,1+\kappa}(2u-1))^2 = \frac{\Gamma(n) \Gamma(n+2+\kappa)}{n! (1+\kappa+2n) \Gamma(1+\kappa+n)} = \frac{(n+1+\kappa)}{n(1+\kappa+2n)}$$

It is easy to check that eigenfunctions of Eq. (3.35) satisfy the following boundary conditions;

$$Z_n(u=0) = 0 ; \quad Z_n(u=1) = 0 \quad (3.37)$$

We found that the easiest way to solve the master equation (see Eq. (3.28)) is to introduce  $Z(Y, u) = u + \tilde{Z}(Y, u)$ . The equation for  $\tilde{Z}$  can be reduced to the Sturm-Liouville form, namely,

$$s(u) \frac{\partial \tilde{Z}}{\partial Y} = \frac{\partial}{\partial u} p(u) \frac{\partial \tilde{Z}}{\partial u} + \Phi(u) \quad (3.38)$$

where

$$s(u) = \frac{1}{u(1-u)} u^{-\kappa} ; \quad p(u) = u^{-\kappa} ; \quad \Phi(u) = -\kappa u^{-\kappa} \quad (3.39)$$

The solution to Eq. (3.38) has the form

$$\tilde{Z}(Y, u) = \int_0^Y dY \int_0^1 d\xi G(Y - y'; u, \xi) \Phi(\xi) \quad (3.40)$$

where

$$G(Y; u, \xi) = \sum_{n=1}^{\infty} \frac{(1 - \exp(-\lambda_n Y))}{\lambda_n} \frac{Z_n(u) Z_n(\xi)}{\|Z_n\|^2} \quad (3.41)$$

where  $\lambda_n$  are given by Eq. (3.34) and  $Z_n$  is the set of the eigenfunction shown in Eq. (3.35).

In Fig. 6 we plotted the energy behaviour of the scattering amplitude for different values of  $u$  that are close to unity. One can see that this solution gives the amplitude which is quite different from the semi-classical solution. It sounds controversial, but actually it is not, since the solution of Eq. (3.40) contains the integral over  $\xi$  from 0 to 1 while our functions  $Z_n$  of Eq. (3.35) we know only at  $u \rightarrow 1$ .

It turns out that we can find a very simple solution at small values of  $u$  ( $u \rightarrow 0$ ). Introducing a new variable  $\gamma = 1 - u$  we can rewrite our master equation in the form at  $\gamma \rightarrow 1$

$$\frac{\partial Z}{\partial \gamma} = (1 - \gamma) \left( \kappa \frac{\partial Z}{\partial \gamma} + \gamma \frac{\partial^2 Z}{(\partial \gamma)^2} \right) \quad (3.42)$$

or in  $\omega$ -representation it looks as

$$\omega Z(\omega, \gamma) = (1 - \gamma) (\kappa Z_\gamma(\omega, \gamma) + \gamma Z_{\gamma\gamma}(\omega, \gamma)) \quad (3.43)$$

The solution to this equation has the form

$$Z(\omega, \gamma) = {}_2F_1(\alpha, \beta, \kappa, \gamma) = {}_2F_1(\alpha, \beta, \kappa, 1 - u) \quad (3.44)$$

where

$$\begin{aligned}\alpha &= \frac{1}{2} \left( \kappa - 1 \right) + \sqrt{(1 - \kappa)^2 - 4\omega} ; \\ \beta &= \frac{1}{2} \left( (\kappa - 1) - \sqrt{(1 - \kappa)^2 - 4\omega} \right) ;\end{aligned}\tag{3.45}$$

The condition that gives us the spectrum of  $\omega$  is

$$Z(\omega, 1 - u = 1) = {}_2F_1(\alpha, \beta, \kappa, 1) = \frac{\Gamma(\kappa) \Gamma(1)}{\Gamma(\kappa - \alpha) \Gamma(\kappa - \beta)} = 0\tag{3.46}$$

The equation for the eigenvalues has the form

$$\kappa - \alpha - n ; \text{ (or } \kappa - \beta - n \text{ ) } \text{ which gives } \omega_n = -\lambda_n = n^2 + n(\kappa + 1) + 1\tag{3.47}$$

One can see that this spectrum practically coincides with Eq. (3.34). Therefore, we can assume that Eq. (3.35) or Eq. (3.34) determines the spectrum of our problem in the entire region of  $u$ . This fact we will use below to develop the numerical approach to the master equation.

### 3.3 Approximate method

The semi-classical solution we can compare with a simpler approximation suggested in Ref. [13]. This approach consists of two steps. The first one is to find the asymptotic solution, namely, the solution to the following equation

$$-\kappa \phi'_u + (\phi'_u)^2 = 0\tag{3.48}$$

This solution is  $\phi_{asympt}(u) = \kappa(u - 1)$  which satisfies the normalization  $\phi(u = 1) = 0$  that follows from  $Z(u = 1, Y) = 1$ . The next step is to find a solution in the form  $\phi(u; Y) = \phi_{asympt}(u) + \Delta\phi(u; Y)$  assuming that  $\Delta\phi(u; Y) \ll \phi_{asympt}(u)$ . The equation for  $\Delta\phi(u; Y)$  is the typical Liouville equation

$$\frac{\partial \Delta\phi(u; Y)}{\partial Y} = \kappa u (1 - u) \frac{\partial \Delta\phi(u; Y)}{\partial u}\tag{3.49}$$

with the initial condition

$$\Delta\phi(u; Y = 0) = \ln(u) - \kappa(u - 1)\tag{3.50}$$

The solution is an arbitrary function of the following type

$$\Delta\phi(u; Y = 0) = H \left( Y + \frac{1}{\kappa} \ln \left( \frac{u}{1 - u} \right) \right)\tag{3.51}$$

which can be found from the initial condition of Eq. (3.50).

The solution has the form

$$Z(u; Y) = \frac{u e^{\kappa Y}}{1 - u + u e^{\kappa Y}} \exp \left( \kappa u (1 - u) \frac{1 - e^{\kappa Y}}{1 - u + u e^{\kappa Y}} \right)\tag{3.52}$$

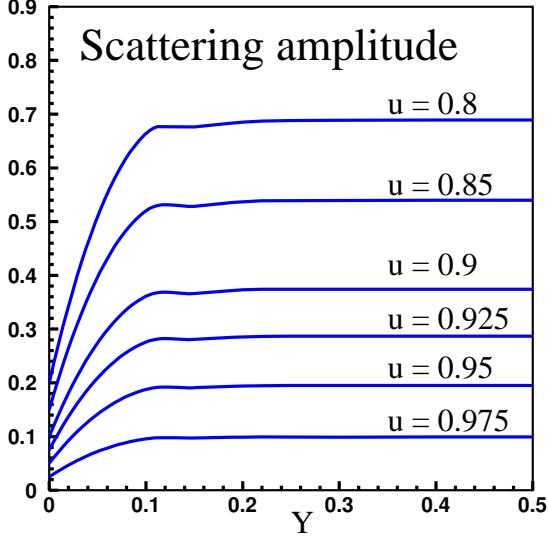


**Figure 6:** The scattering amplitude as a function of rapidity at different values of  $u \rightarrow 1$ .

This solution corresponds to the general solution, given by Eq. (3.25), but only one solution  $\phi^+(\omega, u)$  is taken into account. In spite of the fact that the full semi-classical solution looks quite different from the simple expression of Eq. (3.52) the both solution are in less than 1% agreement at least for  $\mathcal{Y} \geq 0.3$ .

#### 4. The exact solution to the problem

A master equation of Eq. (2.8) we can re-write in more convenient form, introducing a new function  $\mathcal{G}$ , namely,

$$\begin{aligned} Z(\omega, u) &= e^{\frac{\kappa}{2}u} \mathcal{G}(v, \omega) u(1-u) \\ &= \frac{1-v^2}{4} \mathcal{G}(v, \omega) e^{\frac{\kappa}{4}(1-v)} \end{aligned}$$

where  $v = 1 - 2u$  (4.1)

For the function  $G$  we have

$$\omega \mathcal{G}(\omega, v) = -\frac{\kappa^2}{16} (1 - v^2) \mathcal{G}(\omega, v) + ((1 - v^2) \mathcal{G}(\omega, v))_{vv} \quad (4.2)$$

The equation for  $\mathcal{G}$  can be re-written in the form

$$(1 - v^2) \mathcal{G}_{vv} - 4v \mathcal{G}'_v + \left\{ -\omega - 2 - \frac{\kappa^2}{16} (1 - v^2) \right\} \mathcal{G} = 0 \quad (4.3)$$

For function  $S_{n,m} = (1 - v^2)^{\frac{m}{2}} \mathcal{G}(\omega, v)$  Eq. (4.3) reduces to the equation for the oblate spheroidal wave function with the fixed order parameter  $m = 1$  and arbitrary degree parameter  $n$  which is an integer, ( $S_{n,m}(c, v)$  (see Refs. [32, 40]), namely,

$$\frac{d}{dv} (1 - v^2) \frac{dS_{n,m}(c, v)}{dv} + \left( \lambda_n^m - cv^2 - \frac{m^2}{1 - v^2} \right) S_{n,m}(c, v) = 0 \quad (4.4)$$

where

$$\begin{aligned} \omega_n &= -\frac{\kappa^2}{16} - 2 + m(m+1) - \lambda_n^m = -\frac{\kappa^2}{16} - \lambda_n^m ; \\ m &= -1 ; \quad c^2 = -\frac{\kappa^2}{16} ; \end{aligned} \quad (4.5)$$

and the set of the eigenfunctions for the generating function  $Z_n$  is equal to

$$Z_n = (1-v)^{\frac{1}{2}} S_{n,1}(v, i\frac{\kappa}{4}) e^{\frac{\kappa}{4}(1-v)} \quad (4.6)$$

Using Eq. (3.34) for the spectrum of our equation at  $u \rightarrow 1$  as a first approximation for calculation of the eigenvalue  $\lambda_n^{-3}$  we obtain

$$\lambda_n^{(1)} = n^2 + \kappa(n+1) - \frac{\kappa^2}{16} \quad (4.7)$$

The normalization of function  $S_{n,1}$  is given by the following equations [32]

$$\|S_{n,1}(c, v)\|^2 = \int_{-1}^1 dv |S_{n,m}(c, v)|^2 = \frac{2n(n+1)}{2n+1} \quad (4.8)$$

The Green function of Eq. (4.4) has the form

$$G(Y - Y'; v, \xi) = \sum_{n=1}^{\infty} e^{-\lambda_n^1(Y-Y')} \frac{S_{n,1}(i\frac{\kappa}{4}, v) S_{n,1}(i\frac{\kappa}{4}, \xi)}{\|S_{n,1}(i\frac{\kappa}{4}, v)\|^2} \quad (4.9)$$

It should be stressed that the  $Y$  dependence of the Green function is determined by the condition  $E_n - E_{min} = -\omega_n + \omega_0 = \lambda_n^1$  in accordance with the Schroedinger equation (see Eq. (2.37)).  $E_0 = -\omega_0$  is the lowest energy level which corresponds to the asymptotic state of Eq. (2.42). Therefore, Eq. (4.9) explicitly demonstrate that the generating function  $Z$  tends to  $Z \rightarrow Z_{asympt}$  at high energies.

This Green function leads to the following formula for the generating function  $Z(Y, u)$

$$Z(Y, u) = u + \quad (4.10)$$

$$\frac{\sqrt{1-v^2}}{4} e^{\frac{\kappa}{4}(1-v)} \sum_{n=1}^{\infty} \left( \frac{1 - e^{-\lambda_n^1 Y}}{\lambda_n^1} \right) \frac{S_{n,1}(i\frac{\kappa}{4}, v) \int_{-1}^1 d\xi S_{n,1}(i\frac{\kappa}{4}, \xi) \left( -\frac{\kappa^2}{4} \sqrt{(1-v^2)} e^{-\frac{\kappa}{4}(1-\xi)} \right)}{\|S_{n,1}(i\frac{\kappa}{4}, v)\|^2}$$

The spectrum of Eq. (4.7) is correct only at very large value of  $n > \kappa$  since in section 3.2, where we found this spectrum, we actually solved the Schroedinger equation of Eq. (2.37) but with the potential which is plotted in Fig. 2 as a dashed line. It is clear from Fig. 2 that for  $\lambda_n < \kappa$  the spectrum should be different. In particular, we anticipate that all energy levels with these small energies will have the same values reflecting under barrier transition in our potential [39].

Fortunately, we have a rather detailed knowledge of the spheroidal functions in mathematics including the spectrum of  $\lambda_n^1$  (see Refs. [32, 40]). The series in Eq. (3.19) is well converged and, practically, we need to take into account only about 10 terms.

Eq. (4.10) can be easily generalized for arbitrary initial condition:  $Z(Y=0; u) = F(u)$ .

Indeed, the solution has the form

$$Z(Y, u) = F(u) + \quad (4.11)$$

$$\frac{\sqrt{1-v^2}}{4} e^{\frac{\kappa}{4}(1-v)} \sum_{n=1}^{\infty} \left( \frac{1 - e^{-\lambda_n^1 Y}}{\lambda_n^1} \right) \frac{S_{n,1}(i\frac{\kappa}{4}, v) \int_{-1}^1 d\xi S_{n,1}(i\frac{\kappa}{4}, \xi) \left( -\frac{\kappa^2}{4} \frac{L(F(u))}{\sqrt{(1-v^2)}} e^{-\frac{\kappa}{4}(1-\xi)} \right)}{\|S_{n,1}(i\frac{\kappa}{4}, v)\|^2}$$

where  $L$  is the Sturm - Liouville operator defined in Eq. (2.29). In coming papers we will discuss the master equation with different initial conditions that reflect the interaction with nuclei and other targets [41, 42]

## 5. Numerical estimates

In our numerical calculations we use the package for mathematica written by P. Falloon (see Ref. [40] which allows us to compute both the eigenvalues  $\lambda_n^1$  and the spheroidal wave functions  $S_{n,1}$  with fixed  $c$  given by Eq. (4.5). The result of our calculations at fixed  $\kappa = 16$  which is related to the QCD coupling constant  $\alpha_s = 0.25$ , are plotted in Fig. 7 and Fig. 8.

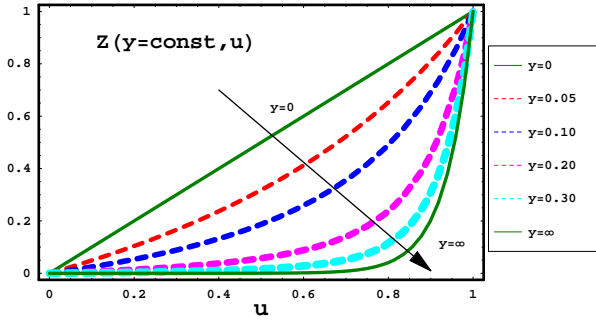


Fig. 7-a

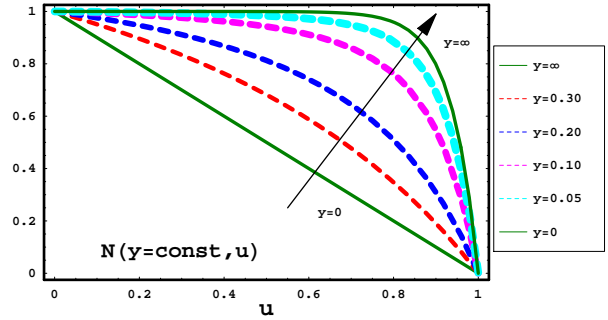


Fig. 7-b

**Figure 7:** The  $u$  dependence for the generating function  $Z(Y, u)$  (Fig. 7-a) and the scattering amplitude  $N(Y, u) = 1 - Z(Y, u)$  (Fig. 7-b) at different values of rapidity. In this figure we plot  $Y \equiv \mathcal{Y}$  (see Eq. (5.1)). At  $Y = \infty$  the asymptotic solution of Eq. (2.42) is shown.

Fig. 7 shows the generating function as function of  $u$  at different energies. One can see that at  $\mathcal{Y} \gg 1$  the solution approaches the asymptotic solution of Eq. (2.42) (the low dashed line in Fig. 7) in accordance with our expectations [39, 38, 13]. To understand the scale of the energy dependence we need to go back to the rapidity  $Y$  from  $\mathcal{Y}$ . As we have discussed

$$Y = \frac{\kappa}{\Gamma(1 \rightarrow 2)} \mathcal{Y} = \frac{1}{\alpha_s^2 \omega_{BFKL}} \mathcal{Y} \quad (5.1)$$

where  $\omega_{BFKL}$  is the intercept of the BFKL Pomeron[3], namely,  $\omega_{BFKL} = 4 \ln 2 \alpha_s$ . For  $\alpha_s = 0.25$  which we use in this paper,  $Y = 23 \mathcal{Y}$ . Therefore,  $\mathcal{Y} = 0.3$  gives  $Y - Y_0 = 6.9$  ( $Y_0$  is the initial rapidity from which we can apply our high energy approximation).

Fig. 8 shows the main result of this paper: the energy (rapidity) dependence of the scattering amplitude. One can see that the exact solution approaches the asymptotic solution as has been foreseen in the approximate solutions to the problem (see, for example, Refs. [39, 38, 13]).

This result eliminates the last uncertainty that the high energy limit of the scattering amplitude does not show the black disc behaviour but we have rather gray disc one as has been discussed before in Ref. [13]. It turns out that at  $\mathcal{Y} \geq 0.5$  ( $Y \geq 12.5$ ) the difference between the exact solution and the asymptotic one is very small. However, for  $\mathcal{Y} \leq 0.5$  the difference between the semi-classical approach and the exact solution is rather large and all approximate methods should be taken with the justified suspicion in this kinematic region.

In appendix B we develop the numerical method specially for small values of  $Y$  and we compare it with the exact solution of Eq. (4.10).

## 6. Conclusions

The core of this paper is the exact analytical solution to the BFKL Pomeron calculus in the zero transverse dimension given in section 4. The method, that we proposed, is very general and can be applied to a various kind of practical problems in future.

The scattering amplitude at high energies, which stems from the exact solution, shows the gray disc behaviour of the asymptotic solution (see Eq. (2.42)). Therefore, we filled the hole in the proof demonstrating that the asymptotic behaviour of Eq. (2.42) satisfies the initial conditions.

We found that the approximations to the master equation, developed in the past (see Refs. [39, 38, 13, 14, 15]), work quite well at large values of rapidity ( $Y \geq 12.5$ ) and can be used in either asymptotic estimates or for an illustration of the main properties of the high energy interaction. The advantage of all of them is their simplicity and transparent physics ideas that are behind these methods. In this respect the semi-classical approach is especially attractive since it gives the clear understanding of the spectrum of the problem and the behaviour of the eigenfunctions. However, the comparison with the exact solution shows that we cannot trust the approximate methods for low energies, namely, for  $Y \leq 12.5$  where there exist the most of the experimental data including ones that we anticipate from the LHC.

We firmly believe that the solution for the BFKL Pomeron calculus at zero transverse dimension is the necessary step in our understanding of the behaviour of the scattering amplitude at high energies in QCD. The real QCD problem is much more complicated but the fact, that we can compare the approximation methods with the exact solution for our toy model and found that they work quite well, might open a way to solve the QCD problem at high energies developing different approximations (see Refs. [21, 22, 13] where one can see the first attempts of such kind of approaches).

## Acknowledgments

### 7. Acknowledgments:

We want to thank Asher Gotsman, Edmond Iancu, Volodya Khachtryan, Uri Maor and Jeremy Miller for very useful discussions on the subject of this paper. The special thanks go to Bo-Wen Xiao for discussion with us the results of Ref. [15].

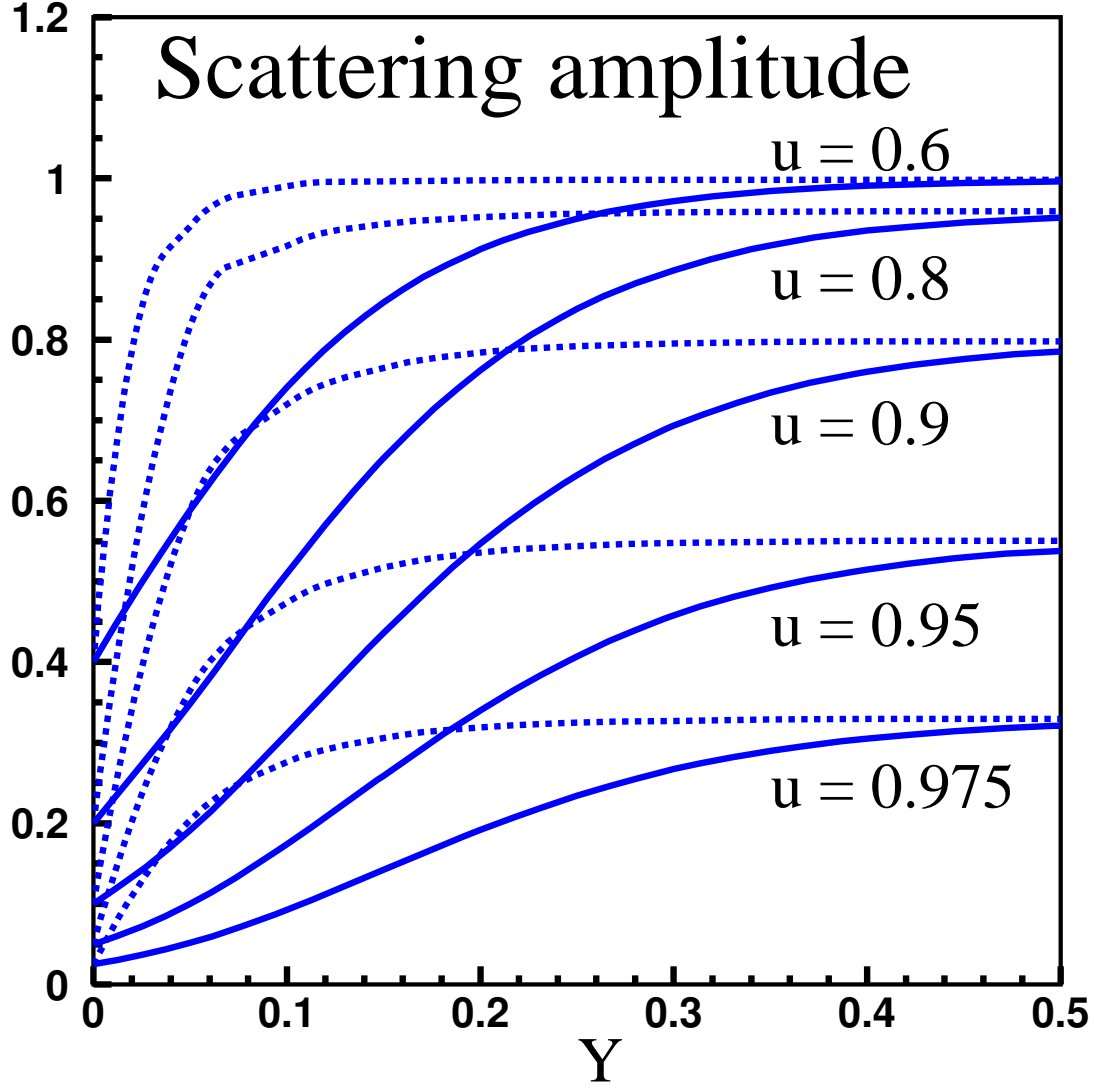


**Figure 8:** The rapidity dependence of the scattering amplitude  $N(Y, u)$  at different values of  $u$ . The dashed curves are the semi-classical solution of Eq. (3.25), while the solid lines are the exact solution to the master equation. In this figure we plot  $Y \equiv \mathcal{Y}$  (see Eq. (5.1)).

This research was supported in part by the Israel Science Foundation, founded by the Israeli Academy of Science and Humanities and by BSF grant # 20004019.

## A. Appendix A: The exact semi-classical solution.

At this appendix we calculate exactly functions  $\phi^\pm(\omega, u)$  for the semi-classical solution (see section 3.1) and compare them with the approximations at small and large values of  $\omega$ , which were used for calculation in this section.

Recall that

$$\phi_u^\pm = \frac{\kappa}{2} \left\{ 1 \pm \sqrt{1 + \frac{4\omega}{\kappa^2 u(1-u)}} \right\} \quad (\text{A.1})$$

Therefore, functions  $\phi^\pm$  (see Eq. (3.1) and Eq. (3.4)) are defined by the following integrals:

$$\phi^\pm(u) = - \int_u^1 \frac{\kappa}{2} \left\{ 1 \pm \sqrt{1 + \frac{4\omega}{\kappa^2 u'(1-u')}} \right\} du' = I_1 + I_2 \quad (\text{A.2})$$

where the first integral is trivial:

$$I_1 = - \int_u^1 \frac{\kappa}{2} du' = \frac{\kappa}{2} (u - 1) \quad (\text{A.3})$$

The second term is a bit more complicated and can be expressed using well known elliptic integrals:

$$I_2 = \mp \frac{\kappa}{2} \int_u^1 \sqrt{1 + \frac{4\omega}{\kappa^2 u'(1-u')}} du' = \mp [II_2(1) - II_2(u)] \quad (\text{A.4})$$

where  $II_2$  defined as following indefinite integral:

$$\begin{aligned} II_2(u) = & -u \cdot \sqrt{1 + \frac{4\omega}{\kappa^2 (1-u)u}} \\ & \frac{(1-u) \sqrt{\frac{1}{2} + \frac{2\omega}{\kappa^2 (1-u)u}} \sqrt{1 - \frac{8\omega + \kappa^2 (1-u)}{\kappa (1-u) \sqrt{\kappa^2 + 16\omega}}} (-8\omega - \kappa (1-u) (k + \sqrt{\kappa^2 + 16\omega}))}{4 (\kappa^2 (1-u)u + 4\omega) \omega \sqrt{1 + \frac{\kappa^2 (1-u) + 8\omega}{\kappa (1-u) \sqrt{\kappa^2 + 16\omega}}}} \\ & \cdot \left\{ \sqrt{\frac{\kappa^2 + 8\omega - \kappa \sqrt{\kappa^2 + 16\omega}}{\omega (1-u)u}} EE \left[ A^-, \frac{2\kappa \sqrt{\kappa^2 + 16\omega}}{\kappa^2 + 8\omega - \kappa (\kappa + \sqrt{\kappa^2 + 16\omega})} \right] \right. \\ & 16\omega \sqrt{\frac{t\omega}{(u-1)(8\omega + \kappa(\kappa + \sqrt{\kappa^2 + 16\omega}))}} EF \left[ A^+, \frac{2\kappa \sqrt{\kappa^2 + 16\omega}}{8\omega + \kappa (\kappa + \sqrt{\kappa^2 + 16\omega})} \right] \\ & \left. 8\omega \sqrt{\frac{u\omega}{(u-1)(\kappa^2 + 8\omega - \kappa(\kappa + \sqrt{\kappa^2 + 16\omega}))}} EF \left[ A^-, \frac{-2\kappa \sqrt{\kappa^2 + 16\omega}}{\kappa^2 + 8\omega - \kappa (\kappa + \sqrt{\kappa^2 + 16\omega})} \right] \right\} \end{aligned} \quad (\text{A.5})$$



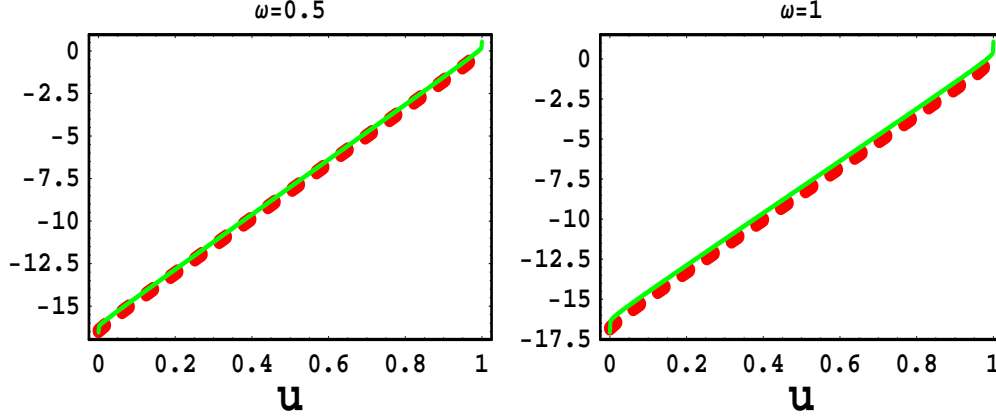


**Figure 9:** This plot shows the exact function  $\phi^+(\omega, u)$  (thick dotted line) and the approximate function  $\phi(\omega)$  of Eq. (3.6) (thin solid line) for small values of  $\omega$  (i.e.  $\omega \leq \kappa^2$ ).  $\kappa = 16$  for the plot.

In the last equation we used the following notations:

$$A^\pm \equiv \arcsin \left( \sqrt{\frac{1}{2} \pm \frac{\kappa^2(1-u) + 8\omega}{2\kappa(1-t)\sqrt{\kappa^2 + 16\omega}}} \right) \quad (\text{A.6})$$

and  $EF(\varphi, m)$  is the elliptic integral of the first kind [31] defined as

$$EF(\varphi, m) \equiv \int_0^\varphi (1 - m \cdot \sin^2(\theta))^{-1/2} d\theta \quad (\text{A.7})$$

while  $EE(\varphi, m)$  is the elliptic integral of the second kind [31]

$$EE(\varphi, m) \equiv \int_0^\varphi (1 - m \cdot \sin^2(\theta))^{+1/2} d\theta \quad (\text{A.8})$$

We can see that, in spite the fact that  $\phi^\pm$  can be calculated explicitly (in radicals), the expression is so complicated that it is difficult to use it for the calculations of the functions  $\Phi^\pm(\omega)$  in Eq. (3.5). Nevertheless, this exact calculation very useful by two reasons: (i) using exact form of  $\phi^\pm$  we can estimate the accuracy of our approximate expression for functions  $\phi^\pm(\omega, u)$ , and (ii) we can find the separation parameter between small and large  $\omega$  that we used in our semi-classical solution of section 3.2.

The plots in Fig. 9 and in Fig. 10 illustrate how good our approach for small and large  $\omega$ , which we used for calculations of  $\phi^\pm$ .

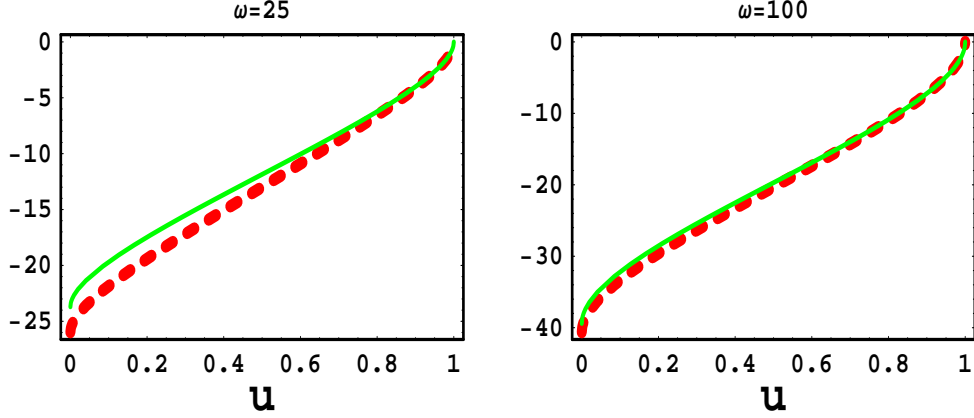


**Figure 10:** This plot shows the exact function  $\phi^+(\omega, u)$  (thick dotted line) and the approximate function  $\phi(\omega)$  of Eq. (3.6) (thin solid line) for large values of  $\omega$  (i.e.  $\omega \geq \kappa^2$ ).  $\kappa = 16$  for the plot.

## B. Appendix B: The exact solution as a power series in rapidity

Our master equation Eq. (2.1) can be solved exactly for the arbitrary initial conditions:  $Z(Y = 0; u) = f(u)$  in terms of the power series of rapidity. This method has a number of exclusive advantages: (I) it applicable for all reasonable initial conditions, which allow us to apply such solution for the different scattering processes at high energies; (II) with this method we can easily solve all modifications of our master equation, which incorporates next order corrections with the only one restriction that the variable coefficients in the diffusion equation can be represented as power series in  $u$ ; (III) this method extremely good for small values of rapidity  $y$  and in vicinity of  $u = 0$  and  $u = 1$  (we will demonstrate this below with numerical calculations). The last argument especially important, since all solutions, which are based on approximate methods, lead to large errors just for small values of rapidity  $y$  and/or in vicinity of  $u = 0$  and  $u = 1$ .

Unfortunately, solution in terms of power series of rapidity is converged relatively slowly, thus this method is not applicable for calculations of the asymptotic behaviors of the scattering amplitude. Nevertheless, we believe that proposed method will be very useful for practical calculations, because most of the experimental data, available now, are concentrated at small or intermediate values of rapidity.

It is very instructive to start with the direct decompositions of function  $Z(\mathcal{Y}, u)$ :

$$Z(\mathcal{Y}, u) = \sum_{n=0}^{\infty} C_n(u) \cdot \mathcal{Y}^n \quad (\text{B.1})$$

It is obviously the first term in such expansion corresponds to appropriate initial conditions, indeed at  $\mathcal{Y} = 0$  we have:

$$Z(\mathcal{Y} = 0, u) = \sum_{n=0}^{\infty} C_n(u) \cdot (\mathcal{Y} = 0)^n = C_0(u) = f(u) \quad (\text{B.2})$$

Now by substitution of Eq. (B.1) into our master equation Eq. (2.1) and after arranging the appropriate powers of  $\mathcal{Y}$  we will get the following recurrence equations for the functions  $C_n(u)$ :

$$C_{n+1}(u) = \frac{u(1-u)}{n+1} \cdot \left[ \frac{\partial^2 C_n(u)}{\partial u^2} - \kappa \frac{\partial C_n(u)}{\partial u} \right] \quad (\text{B.3})$$

Therefore, once we know initial conditions of our problem Eq. (B.2), all series expansions Eq. (B.1) are well defined and can be calculated up to arbitrary order. Finally, introducing the differential operator  $\hat{L}^n$  as follows

$$\hat{L}^i[f(u)] \equiv \hat{L} \left[ \hat{L}^{i-1}[f(u)] \right] ; \quad \hat{L} \equiv \frac{u(1-u)}{n+1} \cdot \left[ \frac{\partial^2}{\partial u^2} - \kappa \frac{\partial}{\partial u} \right] \quad (\text{B.4})$$

the answer can be written in the very elegant form:

$$Z(\mathcal{Y}, u) = f(u) + \sum_{n=1}^{\infty} \hat{L}^n [f(y)] \cdot \mathcal{Y}^n \quad (\text{B.5})$$

This result is nice from the analytical point of view: (1) it haven't singularities, (2) the expansion is well defined for all orders. Nevertheless, for numerical estimations probably not so usefully. The reason for this is clear: series expansion Eq. (B.5) is converged relatively slowly and even more, the radius of convergence is the function of  $u$ . For example, taking first 20 terms of our expansion we can ensure solution  $Z(\mathcal{Y}, u)$  in rapidity rang  $Y \in [0, 5]$ . So from numerical point of view this solution can be considered as solution for small and intermediate values of rapidity.

Fortunately, we can improve numerical property of proposed solution by simple modification, namely we are going expand not the function  $Z(\mathcal{Y}, u)$ , but function  $\varphi(\mathcal{Y}, u) = \ln[Z(\mathcal{Y}, u)]$ . It is obviously that this modification was inspired by our experience in semi-classical solution, but now we are going to keep all terms and propose exact solution.

The first step, which we do is rewriting our master equation Eq. (2.1) in terms of function  $\varphi(\mathcal{Y}, u) = \ln[Z(\mathcal{Y}, u)]$ , by simple substitution we get the following equation for  $\varphi(\mathcal{Y}, u)$ :

$$\frac{\partial \varphi}{\partial \mathcal{Y}} = u(1-u) \cdot \left( \left( \frac{\partial \varphi}{\partial u} \right)^2 + \frac{\partial^2 \varphi}{\partial u^2} - \kappa \frac{\partial \varphi}{\partial u} \right) \quad (\text{B.6})$$

Now one again, we search a solution for this equation in terms of power series of rapidity:

$$\varphi(\mathcal{Y}, u) = \sum_{n=0}^{\infty} B_n(u) \cdot \mathcal{Y}^n \quad (\text{B.7})$$

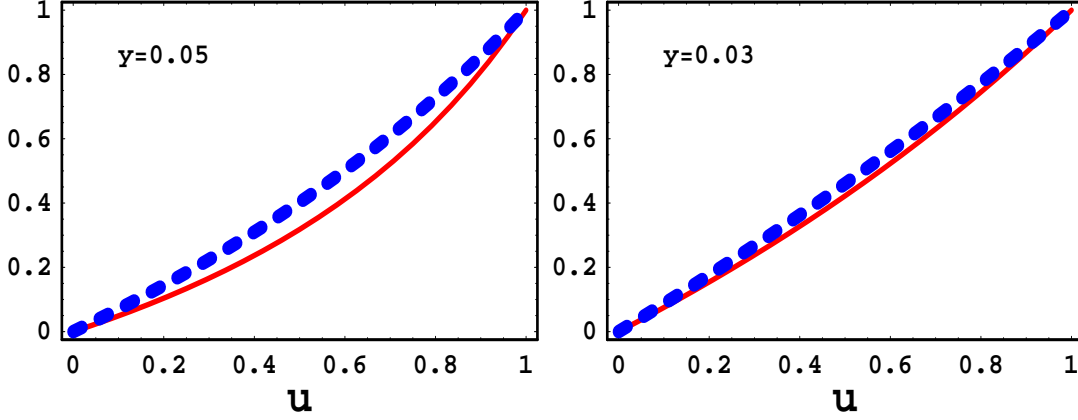


**Figure 11:** In this plot we compare the exact solution of Eq. (4.10) - a solid line and the solution, given by the power series in rapidity, taking into account first 20 terms (see Eq. (B.5)) - a dashed line. This comparison is performed for two different values of rapidity. As we can see from the plots these solutions are close. In principle, the exact solution is a bit steeper than the power series solution, which obviously reflects the fact that we took into account a limited number of terms in this expansion.

Substituting Eq. (B.7) into Eq. (B.6) and arranging the appropriate powers of  $\mathcal{Y}$ , we obtain the following recurrent relations for functions  $B_n(u)$ :

$$B_{n+1}(u) = \frac{u(1-u)}{n+1} \cdot \left[ \sum_{k=0}^n \frac{\partial B_k(u)}{\partial u} \cdot \frac{\partial B_{n-k}(u)}{\partial u} + \frac{\partial^2 B_n(u)}{\partial u^2} - \kappa \frac{\partial B_n(u)}{\partial u} \right] \quad (\text{B.8})$$

The appropriate initial condition for function  $\varphi(\mathcal{Y}, u)$  is also simple in transformation:

$$\varphi(\mathcal{Y} = 0, u) = \sum_{n=0}^{\infty} B_n(u) \cdot (\mathcal{Y} = 0)^n = B_0(u) = \ln[f(u)] \quad (\text{B.9})$$

The last solution numerically is much more stable and, taking first 20 terms of our expansion, we can ensure solution  $Z(\mathcal{Y}, u)$  already in rapidity range  $Y \in [0, 8]$ . It is important to note that proposed logarithmic transformation works well in all cases, except the specific initial conditions:  $Z(\mathcal{Y} = 0, u) = \text{const}$  (fortunately, for our physical environment such initial conditions does not look reasonable).

Finally, we demonstrate the quality of this method comparing it with the exact solution of Eq. (4.10). It is obviously that for small values of rapidity this method work quite well.

### C. Appendix C: The interaction procedure for the spectrum of the problem

In this appendix we show that the iteration procedure that has been described in 2.3, works quite well

Eigenvalues	$\lambda_1$	$\lambda_2$	$\lambda_3$	$\lambda_4$	$\lambda_5$	$\lambda_6$	$\lambda_7$	$\lambda_8$	$\lambda_9$	$\lambda_{10}$
Spheroidal (exact)	13.0	14.13	21.40	28.63	38.45	50.32	64.24	80.19	98.15	118.13
Asymptotic ( $\lambda_n = n^2$ )	1	4	9	16	25	36	49	64	81	100
First iteration	14.25	14.75	21.25	29.75	40.25	52.75	67.25	83.75	102.25	122.75

**Table 1:** The comparison of the first ten eigenvalues of the master equation with the asymptotic estimates and with the first iteration described in section 2.3.

at least for calculations of the eigenvalues for the master equation ( see Eq. (2.1)). Starting with the exact spectrum of the equation at large values of  $n$  (see Eq. (2.16)) and using the set of eigenfunctions we can develop the regular perturbative approach based on Eq. (2.43) with  $U_0(\Theta)$  being the rectangular-well potential and choosing  $V(\Theta) = \frac{\kappa^2}{4} \sin^2 \Theta$ . The corrections to the eigenvalues ( $\Delta\lambda_n$ ) are determined by the simple formula

$$\Delta\lambda_n = \int_0^\pi d\Theta V(\Theta) |\Psi(\Theta)|^2 \quad (\text{C.1})$$

and the resulting

$$\lambda_n = n^2 + \Delta\lambda_n \quad (\text{C.2})$$

One can see from the Table I that this first iteration leads to the eigenvalues which are very close to the exact eigenvalues of the master equation.

From this table we see that the first iteration reproduces correctly the values of the eigenvalues at small  $n$ . Therefore, we can conclude that the iteration procedure, described in section 2.3, gives the way to approach the exact solution with a good accuracy.

## References

- [1] L. V. Gribov, E. M. Levin and M. G. Ryskin, *Phys. Rep.* **100**, 1 (1983).
- [2] A. H. Mueller and J. Qiu, *Nucl. Phys.*, 427 **B 268** (1986) .
- [3] E. A. Kuraev, L. N. Lipatov, and F. S. Fadin, *Sov. Phys. JETP* **45**, 199 (1977); Ya. Ya. Balitsky and L. N. Lipatov, *Sov. J. Nucl. Phys.* **28**, 22 (1978).
- [4] J. Bartels, M. Braun and G. P. Vacca, *Eur. Phys. J.* **C40**, 419 (2005) [arXiv:hep-ph/0412218]; J. Bartels and C. Ewerz, *JHEP* **9909**, 026 (1999) [arXiv:hep-ph/9908454]; J. Bartels and M. Wusthoff, *Z. Phys.* **C66**, 157 (1995); A. H. Mueller and B. Patel, *Nucl. Phys.* **B425**, 471 (1994) [arXiv:hep-ph/9403256]; J. Bartels, *Z. Phys.* **C60**, 471 (1993).

- [5] M. A. Braun, *Phys. Lett.* **B632** (2006) 297 [arXiv:hep-ph/0512057]; arXiv:hep-ph/0504002; *Eur. Phys. J.* **C16**, 337 (2000) [arXiv:hep-ph/0001268]; M. Braun, *Eur. Phys. J.* **C6**, 321 (1999) [arXiv:hep-ph/9706373]; M. A. Braun and G. P. Vacca, *Eur. Phys. J.* **C6**, 147 (1999) [arXiv:hep-ph/9711486].
- [6] H. Navelet and R. Peschanski, *Nucl. Phys.* **B634**, 291 (2002) [arXiv:hep-ph/0201285]; *Phys. Rev. Lett.* **82**, 137 (1999), [arXiv:hep-ph/9809474]; *Nucl. Phys.* **B507**, 353 (1997) [arXiv:hep-ph/9703238].
- [7] J. Bartels, L. N. Lipatov and G. P. Vacca, *Nucl. Phys.* **B706**, 391 (2005) [arXiv:hep-ph/0404110].
- [8] V. N. Gribov, *Sov. Phys. JETP* **26**, 414 (1968) [*Zh. Eksp. Teor. Fiz.* **53**, 654 (1967)].
- [9] A. H. Mueller, *Nucl. Phys.* **B415**, 373 (1994); *ibid* **B437**, 107 (1995).
- [10] E. Levin and M. Lublinsky, *Nucl. Phys.* **A730**, 191 (2004) [arXiv:hep-ph/0308279].
- [11] E. Levin and M. Lublinsky, *Phys. Lett.* **B607**, 131 (2005) [arXiv:hep-ph/0411121].
- [12] E. Levin and M. Lublinsky, *Nucl. Phys.* **A763**, 172 (2005) , arXiv:hep-ph/0501173.
- [13] E. Levin, *Nucl. Phys.* **A763**, 140 (2005), arXiv:hep-ph/0502243.
- [14] P. Rembiesa and A. M. Stasto, *Nucl. Phys.* **B725** (2005) 251 [arXiv:hep-ph/0503223].
- [15] A. I. Shoshi and B. W. Xiao, “Pomeron loops in zero transverse dimensions,” arXiv:hep-ph/0512206.
- [16] L. McLerran and R. Venugopalan, *Phys. Rev.* **D 49**, 2233, 3352 (1994); **D 50**, 2225 (1994); **D 53**, 458 (1996); **D 59**, 09400 (1999).
- [17] I. Balitsky, [arXiv:hep-ph/9509348]; *Phys. Rev.* **D60**, 014020 (1999) [arXiv:hep-ph/9812311] Y. V. Kovchegov, *Phys. Rev.* **D60**, 034008 (1999), [arXiv:hep-ph/9901281].
- [18] E. Levin and K. Tuchin, *Nucl. Phys.* **A693** (2001) 787 [arXiv:hep-ph/0101275]; **A691** (2001) 779 [arXiv:hep-ph/0012167]; **B573** (2000) 833 [arXiv:hep-ph/9908317]; M. Kozlov and E. Levin, *Nucl. Phys.* **A764** (2001) 498 arXiv:hep-ph/0504146.
- [19] E. Iancu, K. Itakura and L. McLerran, *Nucl. Phys.* **A708** (2002) 327 [arXiv:hep-ph/0203137].
- [20] N. Armesto and M. A. Braun, *Eur. Phys. J.* **C20**, 517 (2001) [arXiv:hep-ph/0104038]; M. Lublinsky, *Eur. Phys. J.* **C21**, 513 (2001) [arXiv:hep-ph/0106112]; E. Levin and M. Lublinsky, *Nucl. Phys.* **A712**, 95 (2002) [arXiv:hep-ph/0207374]; *Nucl. Phys.* **A712**, 95 (2002) [arXiv:hep-ph/0207374]; *Eur. Phys. J.* **C22**, 647 (2002) [arXiv:hep-ph/0108239]; M. Lublinsky, E. Gotsman, E. Levin and U. Maor, *Nucl. Phys.* **A696**, 851 (2001) [arXiv:hep-ph/0102321]; *Eur. Phys. J.* **C27**, 411 (2003) [arXiv:hep-ph/0209074]; K. Golec-Biernat, L. Motyka and A. M. Stasto, *Phys. Rev.* **D65**, 074037 (2002) [arXiv:hep-ph/0110325]; E. Iancu, K. Itakura and S. Munier, *Phys. Lett.* **B590** (2004) 199 [arXiv:hep-ph/0310338]. K. Rummukainen and H. Weigert, *Nucl. Phys.* **A739**, 183 (2004) [arXiv:hep-ph/0309306]; K. Golec-Biernat and A. M. Stasto, *Nucl. Phys.* **B668**, 345 (2003) [arXiv:hep-ph/0306279]; E. Gotsman, M. Kozlov, E. Levin, U. Maor and E. Naftali, *Nucl. Phys.* **A742**, 55 (2004) [arXiv:hep-ph/0401021]; K. Kutak and A. M. Stasto, *Eur. Phys. J.* **C41**, 343 (2005) [arXiv:hep-ph/0408117]; G. Chachamis, M. Lublinsky and A. Sabio Vera, *Nucl. Phys.* **A748**, 649 (2005) [arXiv:hep-ph/0408333]; J. L. Albacete, N. Armesto, J. G. Milhano, C. A. Salgado and U. A. Wiedemann, *Phys. Rev.* **D71**, 014003 (2005) [arXiv:hep-ph/0408216]; E. Gotsman, E. Levin, U. Maor and E. Naftali, *Nucl. Phys.* **A750** (2005) 391 [arXiv:hep-ph/0411242].
- [21] E. Iancu and A. H. Mueller, *Nucl. Phys.* **A730** (2004) 460, 494, [arXiv:hep-ph/0308315], [arXiv:hep-ph/0309276].

- [22] M. Kozlov and E. Levin, *Nucl. Phys.* **A739** (2004) 291 [arXiv:hep-ph/0401118].
- [23] J. Jalilian-Marian, A. Kovner, A. Leonidov and H. Weigert, *Phys. Rev.* **D59**, 014014 (1999), [arXiv:hep-ph/9706377]; *Nucl. Phys.* **B504**, 415 (1997), [arXiv:hep-ph/9701284]; J. Jalilian-Marian, A. Kovner and H. Weigert, *Phys. Rev.* **D59**, 014015 (1999), [arXiv:hep-ph/9709432]; A. Kovner, J. G. Milhano and H. Weigert, *Phys. Rev.* **D62**, 114005 (2000), [arXiv:hep-ph/0004014]; E. Iancu, A. Leonidov and L. D. McLerran, *Phys. Lett.* **B510**, 133 (2001); [arXiv:hep-ph/0102009]; *Nucl. Phys.* **A692**, 583 (2001), [arXiv:hep-ph/0011241]; E. Ferreira, E. Iancu, A. Leonidov and L. McLerran, *Nucl. Phys.* **A703**, 489 (2002), [arXiv:hep-ph/0109115]; H. Weigert, *Nucl. Phys.* **A703**, 823 (2002), [arXiv:hep-ph/0004044].
- [24] E. Iancu and D. N. Triantafyllopoulos, *Nucl. Phys.* **A756**, 419 (2005) [arXiv:hep-ph/0411405]; *Phys. Lett.* **B610**, 253 (2005) [arXiv:hep-ph/0501193].
- [25] A. H. Mueller, A. I. Shoshi and S. M. H. Wong, *Nucl. Phys.* **B715**, 440 (2005) [arXiv:hep-ph/0501088].
- [26] E. Iancu, G. Soyez and D. N. Triantafyllopoulos, arXiv:hep-ph/0510094.
- [27] A. Kovner and M. Lublinsky, arXiv:hep-ph/0510047; arXiv:hep-ph/0503155; *Phys. Rev. Lett.* **94**, 181603 (2005) [arXiv:hep-ph/0502119]; *JHEP* **0503**, 001 (2005) [arXiv:hep-ph/0502071]; *Phys. Rev.* **D71**, 085004 (2005) [arXiv:hep-ph/0501198]; “Odderon and seven Pomerons: QCD Reggeon field theory from JIMWLK evolution,” arXiv:hep-ph/0512316.
- [28] Y. Hatta, E. Iancu, L. McLerran and A. Stasto, *Nucl. Phys.* **A762** (2005) 272 [arXiv:hep-ph/0505235]; arXiv:hep-ph/0504182.
- [29] Erich Kamke, “*Differentialgleichungen: Lösungsmethoden und Lösung Bd. 1: Gewöhnliche Differentialgleichungen*,” Stuttgart, Germany, Teubner Verlag, 1983.
- [30] Andrey D. Polyinin, “*Handbook of Linear Differential Equations for Engineers and Scientists*”, Chapman & Hall/CRC, 2002.
- [31] I. Gradstein and I. Ryzhik, “*Tables of Series, Products, and Integrals*”, Verlag MIR, Moskau, 1981.
- [32] M. Abramowitz and I. Stegun, “*Handbook of Mathematical Function*”, Dover Publications, Inc., New York, 1972.
- [33] L. N. Lipatov, *Nucl. Phys.* **B452**, 69 (1995).
- [34] A. H. Mueller and G. P. Salam, *Nucl. Phys.* **B475**, 293 (1996), [arXiv:hep-ph/9605302]; G. P. Salam, *Nucl. Phys.* **B461**, 512 (1996).
- [35] J. Bartels and E. Levin, *Nucl. Phys.* **B387** (1992) 617.
- [36] S. Munier and R. Peschanski, *Phys. Rev.* **D70** (2004) 077503; **D69** (2004) 034008 [arXiv:hep-ph/0310357]; *Phys. Rev. Lett.* **91** (2003) 232001 [arXiv:hep-ph/0309177].
- [37] A. H. Mueller and D. N. Triantafyllopoulos, *Nucl. Phys.* **B640** (2002) 331 [arXiv:hep-ph/0205167]; D. N. Triantafyllopoulos, *Nucl. Phys.* **B648** (2003) 293 [arXiv:hep-ph/0209121].
- [38] K. G. Boreskov, “*Probabilistic model of Reggeon field theory*,” arXiv:hep-ph/0112325 and reference therein.
- [39] D. Amati, M. Le Bellac, G. Marchesini and M. Ciafaloni, *Nucl. Phys.* **B112** (1976) 107; D. Amati, G. Marchesini, M. Ciafaloni and G. Parisi, *Nucl. Phys.* **B114** (1976) 483

- [40] Le-Wei Li, Xiao-Kang Kang and Mook-Seng Leong, “ *Spheroidal Wave Functions in Electromagnetic Theory*”,  
Jon Wiley & Son Inc. 2002.  
P. Falloon, “*Homepage of the Spheroidal Wave Functions.*”  
<http://www.physics.uwa.edu.au/falloon/spheroidal/spheroidal.html>;
- [41] M. Kozlov and E. Levin, *in preparation*.
- [42] V. Khachatryan and E. Levin, *in preparation*.







